

000
001
002
003
004
005
006
007
008
009
010
011
012
013
014
015
016
017
018
019
020
021
022
023
024
025
026
027
028
029
030
031
032
033
034
035
036
037
038
039
040
041
042
043
044
045
046
047
048
049
050
051
052
053

MODEL-AWARE TOKENIZER TRANSFER

Anonymous authors

Paper under double-blind review

ABSTRACT

Large Language Models (LLMs) are trained to support an increasing number of languages, yet their predefined tokenizers remain a bottleneck for adapting models to lower-resource or distinct-script languages. Existing tokenizer transfer methods typically rely on semantic heuristics to initialize new embeddings, ignoring higher-layer model dynamics and limiting transfer quality. We propose Model-Aware Tokenizer Transfer (MATT), a method that incorporates model internals into the tokenizer transfer process. MATT introduces an Attention Influence Modeling (AIM) objective that distills inter-token communication patterns from a source model into a target model with a new tokenizer, providing an efficient warm-up before standard language modeling. Unlike approaches that focus solely on embedding similarity, MATT leverages attention behavior to guide embedding initialization and adaptation. Experiments across diverse linguistic settings show that MATT recovers a large fraction of the original model’s performance within a few GPU hours, outperforming heuristic baselines. These results demonstrate that incorporating model-level signals offers a practical and effective path toward robust tokenizer transfer in multilingual LLMs.

1 INTRODUCTION

Recent advances in large language models (LLMs) have shifted attention from training monolingual models (Jiang et al., 2023; Touvron et al., 2023) to covering an increasing number of languages (Grattafiori et al., 2024; Team et al., 2025). Such multilingual models have become valuable tools for researchers and practitioners working with lower-resource languages. They can be used directly for downstream tasks, help translate English datasets into the target language (Rybäk, 2023), or act as a robust baseline for further adaptation (Ociepa et al., 2024). Our work focuses on the last scenario: adapting an existing LLM to a new language.

A major practical challenge in this setting is that every pretrained model is tied to a fixed tokenizer. Alternative architectures that avoid a predefined vocabulary, such as the Byte-Latent Transformer (Pagnoni et al., 2025) or H-Net (Hwang et al., 2025), are still in the experimental stage and not yet widely adopted. Tokenizers for multilingual models are usually trained to cover many scripts at once and inevitably favor high-resource languages. As a result, lower-resource languages, especially those with distinct alphabets such as Georgian, often receive a very limited share of the vocabulary. This mismatch leads not only to lower accuracy (Ali et al., 2024; Tamang & Bora, 2024), but also to slower processing and inference, which are vital for the end users.

One practical way to mitigate this problem is tokenizer transfer: replacing the original tokenizer of a pretrained model with a new one tailored to the target language and retraining the input and output embeddings (de Vries & Nissim, 2020). Even models not explicitly trained for multilinguality usually contain some cross-lingual knowledge thanks to shared alphabets or accidental language contamination (Blevins & Zettlemoyer, 2022). Consequently, if we can initialize the new embeddings well, much of the original performance can be recovered and used as a strong starting point for continual pretraining. At the same time, we should not expect this process to introduce entirely new linguistic knowledge, since several studies show that most of the model’s knowledge is stored in the feed-forward layers (Dai et al., 2022; Geva et al., 2021; Nichani et al., 2024).

Most existing tokenizer-transfer methods focus almost exclusively on the embedding layer. They construct new embeddings as linear combinations of the original ones, differing mainly in how the combination weights are computed (Minixhofer et al., 2022; Dobler & de Melo, 2023; Remy et al.,

054 2023; 2024; Li et al., 2025). By ignoring the higher layers, these approaches overlook how the model
 055 actually processes tokens. More recent work, such as Zero-Shot Tokenizer Transfer by Minixhofer
 056 et al. (2024), leverages the full model by training a hypernetwork with a language modeling ob-
 057 jective to predict embeddings. While effective, this strategy is computationally demanding because
 058 language modeling requires full forward and backward passes through the model.

059 To overcome these limitations, we introduce **Model-Aware Tokenizer Transfer (MATT)**, a method
 060 that leverages the internal behavior of the pretrained model rather than relying only on surface
 061 semantics. At the core of MATT is **Attention Influence Modeling (AIM)** objective.

062 AIM encourages the model with the new tokenizer to reproduce the inter-token interactions of the
 063 original model’s attention layers. In effect, the original model acts as a teacher, while the model
 064 with the new tokenizer serves as a student that learns to match its attention patterns. This procedure
 065 distills structural knowledge about token relationships directly from the teacher, providing a richer
 066 and more informative initialization than relying on an embedding layer alone.

067 MATT is orthogonal to existing heuristics based on semantic similarity and can be combined with
 068 them. It acts as an efficient warm-up stage before conventional language model pretraining, reducing
 069 the cost of adaptation while preserving model quality.

070 We evaluate MATT by transferring the tokenizers of Gemma 3 (Team et al., 2025) and Qwen 3
 071 (Team, 2025) models to extended versions that increase compression and expand coverage for sev-
 072 eral languages, including English, German, Japanese, Arabic, Swahili, and Ukrainian. Across mul-
 073 tiple settings, MATT consistently recovers a substantial portion of the original model’s performance
 074 on both generative and discriminative tasks, while requiring only a few GPU hours and outperform-
 075 ing heuristic-based transfer methods.

076 Our contributions can be summarized as follows:

- 077 • Attention Influence Modeling (AIM): a novel distillation objective that aligns the attention
 078 dynamics of two models with different tokenizers.
- 079 • Model-Aware Tokenizer Transfer (MATT): an efficient tokenizer-transfer method that ex-
 080 ploits model dynamics instead of relying solely on semantic relationships, achieving state-
 081 of-the-art results with substantially lower computational cost than language modeling ob-
 082 jectives.
- 083 • Comprehensive evaluation: experiments across multiple languages and models demon-
 084 strating the effectiveness and efficiency of MATT.

085 2 RELATED WORK

086 **Large Language Models and Vocabulary Size** Large Language Models are becoming increas-
 087 ingly multilingual. Early open-source models focused almost exclusively on English (Jiang et al.,
 088 2023; Touvron et al., 2023; Almazrouei et al., 2023), but most recent releases include at least several
 089 languages and offer partial support for many more. This shift toward multilinguality has changed
 090 how researchers choose vocabulary size.

091 Studies show that larger vocabularies can improve model quality (Takase et al., 2025; Liang et al.,
 092 2023), but they also slow training and inference. As a result, most current foundation models use
 093 vocabularies of about 100 to 250 thousand tokens, with strongly multilingual models leaning to-
 094 ward the upper end. This sweet spot, first popularized by XLM-ROBERTa (Conneau et al., 2020),
 095 continues in more recent models such as Gemma (Team et al., 2025), Aya Expanse (Dang et al.,
 096 2024), and even GPT-5¹. Going beyond this range rarely pays off: performance gains are small,
 097 and efficiency drops sharply. As a result, tokenizers cannot achieve an optimal compression rate for
 098 every language, creating a need for techniques that allow efficient transfer of tokenizers to specific
 099 languages or domains without requiring very large vocabularies.

100 **Heuristics-Based Embedding Initialization Methods** When transferring a tokenizer to a new
 101 language or domain, the main challenge is initializing embeddings for tokens that did not exist in

1¹<https://github.com/openai/tiktoken>

108 the original model. Early work on tokenizer transfer (Artetxe et al., 2020; Gogoulou et al., 2022;
 109 de Vries & Nissim, 2020) focused on proving that transfer was possible, so embedding initialization
 110 received little attention. Simple strategies were used, including random initialization, taking the
 111 mean of existing embeddings, sampling from their distribution, copying the embedding of a random
 112 token, or using token frequency as a guide.

113 Later research began to exploit semantic relationships between tokens. WECHSEL (Minixhofer
 114 et al., 2022) was an influential step: it trained FastText (Bojanowski et al., 2017) embeddings for the
 115 source and target languages and used a translation vocabulary to identify the closest source tokens
 116 for each new token. New embeddings were then initialized as weighted averages of these source
 117 embeddings. Several methods followed a similar direction. OFA (Liu et al., 2024) and Tik-to-
 118 Tok (Remy et al., 2023) refined the idea of using cross-lingual similarities, while Transtokenization
 119 (Remy et al., 2024) created its own token-level translation dictionary with FastAlign (Dyer et al.,
 120 2013). Hyper-OFA (Özeren et al., 2025) went further by training a hypernetwork to map tokens from
 121 an external multilingual space into the model’s embedding space, avoiding the need for simplistic
 122 linear combinations. TokAlign (Li et al., 2025) took a co-occurrence perspective, training two GloVe
 123 (Pennington et al., 2014) models on the same corpus to learn a one-to-one alignment matrix between
 124 tokens.

125 As LLMs became more multilingual, overlap between source and target vocabularies became an im-
 126 portant resource. FOCUS (Dobler & de Melo, 2023) trains a FastText model on text tokenized with
 127 the target vocabulary, then initializes new embeddings as similarity-weighted averages of overlap-
 128 ping tokens. CLP Transfer (Ostendorff & Rehm, 2023) takes advantage of topological similarities of
 129 the latent space across model sizes within the same family: embeddings are first trained on a smaller
 130 related model and then aligned to the target model by measuring similarities with overlapping to-
 131 kens.

132 **Beyond Heuristics** While heuristics provide a practical starting point, they have limitations. An
 133 alternative is to train new embeddings directly by continuing language modeling with all other pa-
 134 rameters frozen (de Vries & Nissim, 2020), but this is computationally costly.

135 Mini-Model Adaptation (Marchisio et al., 2023) reduces the cost by using only a subset of layers
 136 and training the embeddings on a language modeling task. Other work (Chen et al., 2023) shows that
 137 periodically resetting embeddings during pretraining makes models more robust to them, reducing
 138 the effort needed to learn new tokens afterwards.

139 Another approach by Minixhofer et al. (2024) trains a universal hypernetwork for a given language
 140 model by sampling tokenizers from a diverse distribution during the language modeling stage. Once
 141 the hypernetwork is trained, we can initialize embeddings for various tokenizers effortlessly, achiev-
 142 ing a solid baseline for further continual pretraining. However, training such a hypernetwork is a
 143 compute-heavy task, requiring forward and backward passes through the whole model in every step
 144 to update the hypernetwork weights, limiting its practicality in settings where we already have a
 145 defined target tokenizer and the trained hypernetwork is not available beforehand.

146

147

148 3 METHOD

149

150 3.1 INTUITION

151

152

153 Large Language Models generate text one token at a time. Decoder-only transformers, which form
 154 the backbone of most modern LLMs, follow the following steps: the embedding of the most recently
 155 generated token is passed through a stack of attention and feed-forward layers, and finally projected
 156 by the LM head to produce a probability distribution over the next token.

157

158

159

160

161

157 Assuming the input embedding of the last token is correct, the feed-forward layers will not damage
 158 its representation. The main source of potential distortion lies in the attention layers, where each
 159 token interacts with the context. Changing the tokenizer introduces new tokens into the context,
 160 altering these interactions and thus the internal representations that drive next-token prediction. Our
 161 goal is to train a model using a new tokenizer so that, despite these changes, its attention layers
 produce output embeddings similar to those generated by the original tokenizer.

162 3.2 PREREQUISITES
163164 Consider an input string s and a tokenization function T , which produces a token sequence $T(s) =$
165 (t_1, t_2, \dots, t_n) of length n .166 In each attention layer², the inputs are the query (\mathbf{Q}), key (\mathbf{K}), and value (\mathbf{V}) state matrices, pro-
167 ducing the output state matrix (\mathbf{O}). Each of these can be seen as a collection of vector states for
168 every token t_i :

170
$$\mathbf{Q} = \begin{bmatrix} \mathbf{q}_1 \\ \mathbf{q}_2 \\ \vdots \\ \mathbf{q}_n \end{bmatrix}_{n \times h} \quad \mathbf{K} = \begin{bmatrix} \mathbf{k}_1 \\ \mathbf{k}_2 \\ \vdots \\ \mathbf{k}_n \end{bmatrix}_{n \times h} \quad \mathbf{V} = \begin{bmatrix} \mathbf{v}_1 \\ \mathbf{v}_2 \\ \vdots \\ \mathbf{v}_n \end{bmatrix}_{n \times h} \quad \mathbf{O} = \begin{bmatrix} \mathbf{o}_1 \\ \mathbf{o}_2 \\ \vdots \\ \mathbf{o}_n \end{bmatrix}_{n \times h},$$

171
172
173
174

175 where h is the hidden size.

176 Attention is computed as:

178
$$\mathbf{O} = \text{Attention}(\mathbf{Q}, \mathbf{K}, \mathbf{V}) = \text{softmax}\left(\frac{\mathbf{Q}\mathbf{K}^T}{\sqrt{d_k}}\right)\mathbf{V} = \mathbf{AV},$$

179
180

181 where \mathbf{A} is the attention matrix of shape $n \times n$, that contains weights with which the value states
182 are aggregated into the output state.183 We can break down the final matrix multiplication \mathbf{AV} into a chain of value states (\mathbf{V}) averages for
184 each token, weighted by the attention matrix \mathbf{A} . The output state for the token t_i would then look
185 the following way:

187
$$\mathbf{o}_i = \text{softmax}\left(\frac{\mathbf{q}_i \mathbf{K}^T}{\sqrt{d_k}}\right)\mathbf{V} = \mathbf{A}_{i,:}\mathbf{V} = \sum_{j=1}^n \mathbf{A}_{i,j} \mathbf{v}_j = \sum_{j=1}^n \mathbf{v}_{i,j}^*,$$

188
189
190

191 where $\mathbf{v}_{i,j}^* = \mathbf{A}_{i,j} \mathbf{v}_j$ is a weighted value state for the token t_j given the query token t_i .193 3.3 SEGMENT-LEVEL INTERPRETATION OF ATTENTION
194195 To compare attention outputs across different tokenizers, we introduce a segmentation function S
196 that splits the input string s into segments (s_1, s_2, \dots, s_m) while respecting a set of tokenization
197 functions \mathcal{T} :

198
$$S(s; \mathcal{T}) = (s_1, s_2, \dots, s_m), \text{ such that}$$

199
$$\forall T \in \mathcal{T} : T(s_1) \circ T(s_2) \circ \dots \circ T(s_m) = T(s),$$

200
201

202 where \circ is a concatenation operator. This ensures that no segment boundary lies within any token
203 produced by any tokenization function in \mathcal{T} .204 The most intuitive approach is a function that splits the input string into words, and the rest of the
205 section is explained in relation to this function. However, for some languages, word segmentation
206 can be ambiguous; thus, in practice, we define our segmentation function to always choose segments
207 of minimal length that still satisfy the above condition (see Appendix A for the algorithm).208 Given S , we define weighted value states for a segment s_k with respect to a query token t_i :

210
$$\mathbf{s}_{i,k} = \sum_{\{j : t_j \in T(s_k)\}} \mathbf{v}_{i,j}^*$$

211
212

213 The output state for token t_i can then be expressed as a sum over segments:214
215 ²While we proceed with a single-head definition, it is directly applicable to multi-head, multi-query, or
grouped-query attention variants.

216
217
218
219
220

$$\mathbf{o}_i = \sum_{j=1}^n \mathbf{v}_{i,j}^* = \sum_{j=1}^m \mathbf{s}_{i,j}$$

221 To move from token-level to segment-level interpretation, we replace individual query tokens with
 222 segment representations. Since the output state of each token is designed to predict the next token,
 223 it is natural to require that the output state of a segment should similarly carry enough information
 224 to predict the next segment. Because the language modeling head still operates at the token level,
 225 we approximate "predicting the next segment" by predicting the first token of that next segment.

226 Consider a segment s_i whose tokens are $T(s_i) = (t_a, t_{a+1}, \dots, t_b)$. The final token t_b produces
 227 the output state used to generate the next token t_{b+1} , which begins the following segment s_{i+1} . We
 228 therefore define a function ℓ_T that maps a segment index to the index of its last token:

229

$$\ell_T(i) = b$$

230
231

The query state of segment s_i is set equal to the query state of its last token:

232

$$\mathbf{q}_i = \mathbf{q}_{\ell_T(i)} = \mathbf{q}_b,$$

233
234
235
236

and the output state of the segment is computed from this query state:

237
238
239
240
241
242

$$\mathbf{o}_i = \text{softmax} \left(\frac{\mathbf{q}_i \mathbf{K}^T}{\sqrt{d_k}} \right) \mathbf{V} = \text{softmax} \left(\frac{\mathbf{q}_{\ell_T(i)} \mathbf{K}^T}{\sqrt{d_k}} \right) \mathbf{V} = \mathbf{o}_{\ell_T(i)} = \sum_{j=1}^m \mathbf{s}_{\ell_T(i),j}$$

243
244

3.4 ATTENTION INFLUENCE MODELING

245
246
247

As described in the Section 3.1, our goal is to train the model with a new tokenizer T' so that its output states match those of the original model with tokenizer T .

248
249
250
251

Since we can enforce a common segmentation function S , we approximate this by requiring the new model to produce the same segment-level outputs \mathbf{o}'_i as the old ones – \mathbf{o}_i . A more detailed objective also matches the weighted value states $\mathbf{s}_{\ell_T(i),j}$ and $\mathbf{s}'_{\ell_{T'}(i),j}$ of every segment s_j for each query segment s_i , with the causal constraint $j \leq i$.

252
253

Given the above, we define the **Attention Influence Modeling** objectives (normal and simplified):

254
255
256
257

$$\mathcal{L}_{AIM} = \frac{2}{m(m+1)} \sum_{i=1}^m \sum_{j=1}^i \mathcal{L}^*(\mathbf{s}_{\ell_T(i),j}, \mathbf{s}'_{\ell_{T'}(i),j}),$$

258
259
260
261

$$\mathcal{L}_{AIM^*} = \frac{1}{m} \sum_{i=1}^m \mathcal{L}^*(\mathbf{o}_i, \mathbf{o}'_i),$$

262
263

where $\mathcal{L}^*(\mathbf{x}, \mathbf{y})$ can be any loss function, that brings \mathbf{x} and \mathbf{y} closer. In Section 4, we experiment with MSE and Cosine Embedding losses.

264
265
266
267

Figure 1 illustrates an example of applying AIM to the text *CH4 – formula for methane*. In this case, we use a word segmentation function together with different tokenization functions for a given query state \mathbf{q}_5 , where the segment s_5 corresponds to `_methane`.

268
269

Figure 2 presents the attention alignment matrix for the same text, where the weighted value states $\mathbf{v}_{i,j}^*$ are grouped into segments. These segment-level representations are then matched and optimized to be equal under the \mathcal{L}_{AIM} loss.

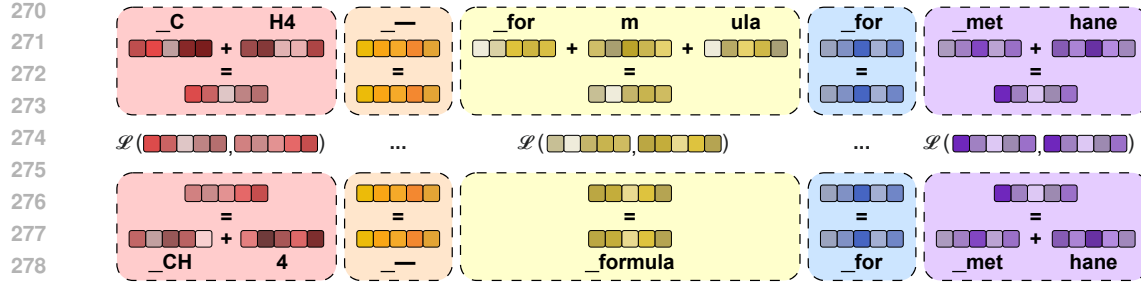


Figure 1: Attention Influence Modeling (AIM) objective with word segmentation. For each input, the weighted value vectors $v_{i,j}^*$ of the original tokens t_j are aggregated into segment-level vectors $s_{i,k}$ according to a chosen word-segmentation function. The model trained with the new tokenizer produces its own segment representations $s'_{i,k}$. The AIM objective encourages these new segment representations to stay close to the segment representations $s_{i,k}$ computed from the model using the old tokenizer. All this happens with respect to the query state q_5 of the 5th segment (_methane), which is equal to the query state of its last token – hane.

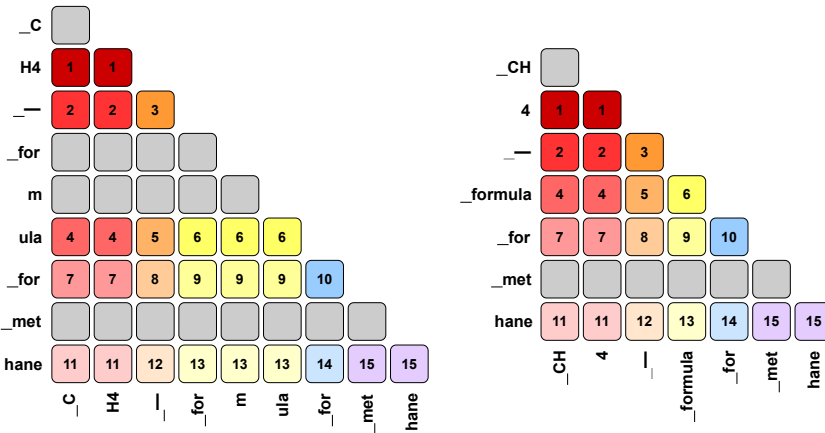


Figure 2: Token-level attention alignment between teacher and student models. The left matrix shows the weighted value states of the teacher model using the original tokenizer T , and the right matrix shows those of the student model using the new tokenizer T' . Each square represents the weighted value state $v_{i,j}^*$ of t_j for query token t_i (i for rows, j for columns). Numbers (or matching colors) within a matrix identify tokens that are aggregated into the same segment-level state $s_{i,k}$. Numbers (or matching colors) across the two matrices indicate corresponding pairs $s_{\ell_T(i),j}$ and $s'_{\ell_{T'}(i),j}$ used in the loss \mathcal{L}^* to align the teacher and the student attention representations.

3.5 TECHNICAL DETAILS

During training, the model with the old tokenizer T is kept frozen. The model with the new tokenizer T' has all layers frozen except the input embeddings. As a small modification to the basic training setup, we partially freeze the embedding matrix: tokens that are shared between the old and new tokenizers are initialized from the original model and kept fixed, while only the embeddings of new, non-overlapping tokens are updated during training.

To speed up convergence, we initialize new embeddings using FOCUS (Dobler & de Melo, 2023). We train with AdamW (Loshchilov & Hutter, 2017), a constant learning rate of 1×10^{-4} , and no weight decay. However, it should be noted that we have not performed extensive hyperparameter tuning, so using learning rate scheduling, adapting the learning rate, weight decay, and other hyperparameters may yield significantly better results.

MATT offers a key advantage over standard language modeling with frozen non-embedding parameters: greater efficiency. Since AIM is defined at the attention-layer level, we can decide how much

324 of the model to include in the tokenizer transfer by selecting the layer depth at which AIM is applied.
 325 Specifically, by choosing a value of n , we take only the first n layers into account. This allows us to
 326 balance efficiency and performance.

327 We ablate the choice of MATT target layer in Appendix C and observe that using higher layers
 328 improves performance until roughly the first quarter of the model, aligning with the formation of
 329 coherent word-level representations as tokens are detokenized in early and middle layers, a behavior
 330 noted in prior work as detokenization (Kaplan et al., 2024). Targeting the final layers causes slight
 331 degradation, consistent with trends reported in Token Distillation Dobler et al. (2025), while middle
 332 layers show a performance plateau. Because later target layers increase training time and memory
 333 linearly (validated in our appendix ablations), we select one of the earliest layers within this plateau
 334 to balance strong performance with minimal resource cost.

335 Since only input embeddings are trained, tied input–output embeddings are advantageous, as the
 336 tuned input embeddings can be reused in the LM head. Models without tied embeddings still benefit
 337 from input tuning, but to a significantly lesser extent; handling untied settings is left for future work.

339 4 EXPERIMENTS

340 We conducted a series of experiments across different languages, model families, and scales to
 341 evaluate the effectiveness of the MATT method compared to existing heuristic- and optimization-
 342 based approaches. In each experiment, we first trained a tokenizer with a higher compression rate
 343 than the original one, merged it with the base tokenizer, and then applied tokenizer transfer to the
 344 extended vocabulary. We have chosen Ukrainian as a language with Cyrillic alphabet that is not well
 345 represented in the dictionaries of the major LLMs and on the other hand that is included in multiple
 346 benchmarks, allowing for the inspection of the method’s performance in different scenarios. For
 347 the multilingual setting we have chosen five typologically diverse languages – English, German,
 348 Japanese, Arabic, and Swahili, which vary in resource availability, writing system, and language
 349 family.

350 Additional experiments, including convergence speed tests (Appendix B) and ablation studies (Ap-
 351 pendix C), are presented to complement the main results.

354 4.1 MAIN RESULTS

355 Our primary evaluation uses the Gemma 3 12B PT model (Team et al., 2025). We replaced its default
 356 tokenizer with an extended version that improves Ukrainian coverage, raising the compression rate
 357 from 2.98 to 4.44. This increase translates to an almost 50% speedup during inference. We compare
 358 the following methods:

- 360 • **WECHSEL** – transfer using the English–Ukrainian vocabulary from the official imple-
 361 mentation³.
- 362 • **Transtokenizers** – token alignment via FastAlign using parallel corpora (OpenSub-
 363 titles (Lison & Tiedemann, 2016) and NLLB (NLLB Team, 2022)) and the official
 364 `transtokenizers`⁴ toolkit.
- 365 • **TokAlign** – GloVe embeddings trained on 2 million Ukrainian documents (approximately
 366 1.86 billion Gemma tokens) from the Kobza corpus (Haltiuk & Smywiński-Pohl, 2025),
 367 used to create a one-to-one alignment matrix with the official implementation⁵.
- 368 • **FOCUS** – FastText embeddings trained on the same data as TokAlign, with initialization
 369 performed via the `deepfocus`⁶ package.
- 370 • **NTP** – initialized with one of the above methods, and trained using the Next Token Predic-
 371 tion (NTP) objective with non-embedding layers frozen. We compare several versions of
 372 this baseline corresponding to 50%, 100%, and 150% of the training budget dedicated to
 373 MATT.

374 ³<https://github.com/CPJKU/wechsel>

375 ⁴<https://github.com/LAGoM-NLP/transtokenizer>

376 ⁵<https://github.com/ZNLP/TokAlign>

377 ⁶<https://github.com/konstantinjdobler/focus>

378 • **MATT** – initialized with FOCUS embeddings and trained on around 240 million Ukrainian
 379 tokens from Kobza using the AIM objective with MSE loss on the 12th layer out of 34,
 380 original embeddings are frozen, and all other hyperparameters remain unchanged (see Sec-
 381 tion 3.5).

383 We evaluate performance on Belebele (Bandarkar et al., 2024), Global MMLU (Singh et al., 2025),
 384 Long FLORES (Paniv, 2025), a modification of FLORES (NLLB Team, 2022; Goyal et al., 2021;
 385 Guzmán et al., 2019), which elevates the sentence-level translation to document-level by aggregating
 386 data points from the same sources, WMT24++ (Deutsch et al., 2025), and XL-SUM (Hasan et al.,
 387 2021). We only evaluate the translations from English to Ukrainian with a specific intent to validate
 388 the model’s performance on a generative task in the target language. Evaluation is performed with
 389 the lm-evaluation-harness framework (Gao et al., 2024) with a 3-shot prompt.

390 Table 1: Performance of Gemma 3 12B PT model with different tokenizer transfer methods on
 391 Bellebele and Global MMLU (accuracy, %), Long FLORES, WMT, and XL-SUM (BLEU). The
 392 ”Avg Disc” column reports the average of Belebele and Global MMLU scores, as well as ”Avg
 393 Gen” – of Long FLORES, WMT, and XL-Sum.

Model	Training Time	Belebele	Global MMLU	Long FLORES	WMT	XL-Sum	Avg Disc	Avg Gen
Gemma 3 12B PT	-	89.33	67.03	14.36	3.52	6.52	78.18	8.13
Heuristics								
WECHSEL	-	22.67	24.61	0.00	0.00	0.00	23.64	0.00
Transtokenizers	-	61.89	46.03	0.04	0.09	0.02	53.96	0.05
TokAlign	-	31.44	32.98	0.00	0.00	0.01	32.21	0.00
FOCUS	-	48.78	37.14	1.01	0.88	0.20	42.96	0.70
Optimization Based								
Transtokenizers w/ NTP	3h 30m	82.44	59.02	3.64	0.88	4.06	70.73	2.86
Transtokenizers w/ NTP	7h 00m	85.22	59.83	4.63	0.95	4.80	72.53	3.46
Transtokenizers w/ NTP	10h 30m	85.67	59.38	5.13	0.96	4.80	72.53	3.63
FOCUS w/ NTP	3h 30m	85.44	57.38	3.51	2.13	4.32	71.41	3.32
FOCUS w/ NTP	7h 00m	87.00	60.55	4.32	2.51	5.04	73.78	3.96
FOCUS w/ NTP	10h 30m	87.44	60.57	4.34	2.60	5.16	74.01	4.03
MATT	7h 00m	89.56	64.98	8.70	4.71	5.95	77.27	6.45

411 Table 1 shows a clear advantage of MATT over all other methods. While heuristic-based approaches
 412 such as FOCUS and Transtokenizers can regain up to about 70% of the original model’s accuracy
 413 on discriminative tasks, they reach no more than about 9% of the original generative performance.

415 Optimization-based approaches show substantially stronger recovery. Among them, NTP yields
 416 consistent results across different heuristic initializations. In its best configuration, NTP recovers
 417 nearly 95% of the original model’s discriminative performance, though only about 50% of its gener-
 418 ative capabilities. In contrast, MATT restores nearly 80% of the original generative performance
 419 while maintaining accuracy on discriminative tasks close to the unmodified model. These results
 420 demonstrate the superiority of the model-aware approach to tokenizer transfer, particularly given
 421 the extremely low computational costs required.

422 The most notable observation is the minimal improvement of NTP when comparing 100% and
 423 150% compute budgets (7 hours and 10.5 hours of training time respectively). NTP training rapidly
 424 saturates, and MATT-level performance does not appear to be attainable within a reasonable budget.
 425 We therefore stop further training due to our limited computational resources.

426 MATT also saturates quickly (see Appendix B), but at a substantially higher performance level. We
 427 hypothesize that further gains are unlikely under embedding-only training and will require unfreez-
 428 ing the model’s layers. This is largely driven by the scale of newly introduced tokens (over 80,000),
 429 which meaningfully alters model dynamics and would likely benefit from full fine-tuning. Due to
 430 computational constraints, we have conducted only limited experiments with continual pretraining
 431 after MATT that provide early support for this hypothesis. A systematic comparison of embedding-
 only adaptation and full model fine-tuning remains a direction for future work.

432 4.2 MULTILINGUAL RESULTS
433

434 In the multilingual setting, we experiment with Gemma 3 4B PT and Qwen 3 0.6B (Team, 2025).
 435 As shown in Table 2, the extended tokenizers consistently improve compression rates across all
 436 languages, including modest gains for English, which directly translates to their processing and
 437 generation speed, since a considerably smaller number of tokens is required to represent the same
 438 text.

439
 440 Table 2: Comparison of original and extended tokenizers. Compression rate is the average number
 441 of characters represented by a single token (higher is better).

Tokenizer	Vocabulary Size	Compression Rate				
		ar	de	en	ja	sw
Gemma						
original	262,145	2.8457	3.9734	4.3187	1.6846	2.9802
extended	387,980	3.9122	4.4997	4.3383	2.1267	4.2518
Qwen						
original	151,669	2.5982	3.4737	4.3599	1.4852	2.5788
extended	298,833	3.9221	4.4886	4.4233	2.2867	4.2322

453 The transfer methods remain the same as in Section 4.1, except the training data is now drawn
 454 from HPLT 2.0 Cleaned (Burchell et al., 2025). FOCUS uses 2 million documents (approximately
 455 500 million tokens per language), and MATT – only about 50 million tokens per language. We
 456 also experiment with an AIM* objective, Cosine Embedding loss, and training without freezing the
 457 original embeddings. Performance is reported on Belebele, MMMLU (Hendrycks et al., 2020), and
 458 Global MMLU. We additionally record the time and memory required to tune embeddings on a
 459 single H100 GPU.

460
 461 Table 3: Benchmark results for transferring original tokenizers to their extended versions across five
 462 languages (Arabic, German, English, Japanese, Swahili). For the proposed MATT method, peak
 463 VRAM usage and processing time required for the tokenizer transfer are also reported.

Model	VRAM GiB	Time	Belebele					MMMLU					Global MMLU					Avg
			ar	de	en	ja	sw	ar	de	en	ja	sw	ar	de	en	ja	sw	
Gemma 3 4B PT	-	-	69.33	68.00	82.00	67.44	59.67	39.24	43.77	53.89	41.20	35.71	45.25	47.50	59.00	47.25	38.00	53.15
FOCUS	-	-	32.89	52.44	80.33	42.00	25.56	27.89	36.89	53.81	32.77	28.23	30.25	36.75	59.50	33.00	26.75	39.94
MATT	16.6	4h 47m	62.44	72.56	80.67	58.00	54.67	37.05	44.79	53.82	38.68	36.10	40.50	47.50	60.25	40.00	39.50	51.10
w/ AIM*	10.9	3h 44m	63.78	70.33	80.78	56.11	54.89	37.22	44.17	53.86	39.15	35.69	37.75	45.50	59.75	40.50	42.25	50.78
w/ cosine	15.7	5h 01m	62.00	70.56	80.67	60.22	59.00	38.33	44.84	53.88	40.48	36.22	42.00	45.25	60.00	41.50	41.75	51.78
w/ unfrozen	20.4	5h 34m	59.78	68.78	80.56	56.22	55.89	38.24	44.77	53.96	40.97	37.95	40.25	48.50	60.00	45.00	41.75	51.51
Qwen3 0.6B	-	-	50.78	59.33	64.11	58.67	29.89	36.08	40.12	47.21	37.54	28.68	38.25	42.75	50.25	44.25	28.25	43.74
FOCUS	-	-	27.11	32.22	60.33	29.22	24.89	28.76	30.28	41.85	29.53	26.58	26.00	31.25	45.25	28.00	24.50	32.38
MATT	9.4	3h 38m	36.67	43.22	60.44	39.44	28.22	32.78	35.14	42.41	33.19	26.71	29.25	35.50	45.25	30.50	25.75	36.30
w/ AIM*	3.5	2h 45m	40.56	45.89	60.44	42.11	28.44	33.15	35.71	42.29	33.72	27.19	32.50	37.00	45.50	37.50	22.75	37.65
w/ cosine	8.6	3h 52m	39.89	46.67	60.33	43.22	28.89	32.77	35.76	42.28	33.41	27.38	33.50	35.75	45.50	35.25	24.50	37.67
w/ unfrozen	10.2	3h 38m	42.22	47.56	62.11	42.89	27.89	33.02	36.46	43.91	33.75	27.50	31.50	38.00	46.25	35.50	24.00	38.17

474
 475 Table 3 shows that MATT substantially narrows the performance gap between a freshly initialized
 476 model and the original, recovering most of the accuracy and occasionally surpassing the original.

477 Regarding the training objectives, the Cosine Embedding loss generally provides strong performance
 478 across the discriminative benchmarks reported in Table 3. However, we note from preliminary
 479 experiments that Mean Squared Error (MSE) tends to be more beneficial for generation-heavy tasks,
 480 and therefore stands as our default choice.

481 A critical observation regarding the effectiveness of MATT is its behavior when the base model
 482 exhibits near-random performance. As a self-distillation method, MATT is designed to recover the
 483 original model’s capabilities rather than induce cross-lingual transfer for unseen languages. This is
 484 evident in the results for Qwen3 0.6B on Swahili. Although the Qwen 3 family technically supports
 485 Swahili, the 0.6B model shows minimal difference from random baselines, likely due to limited
 model capacity and a small share in pretraining data mixture. Despite this unfavorable setting,

486 MATT successfully recovers the majority of the original model’s performance, effectively leveraging
 487 a weak original signal.
 488

489 We also find that the choice of freezing embeddings has an impact on performance depending on
 490 the adaptation scope. Unfreezing all embeddings yields the best results in this multilingual setting.
 491 We attribute this to the need for greater model elasticity when adapting to five diverse languages
 492 simultaneously. In contrast, freezing the original embeddings, as done in Section 4.1, remains the
 493 practical choice for single-language adaptation, where the priority is often to preserve performance
 494 on the original language (e.g., English) while extending coverage to another target language.
 495

496 Based on these findings, we recommend distinct default configurations: for single-language adap-
 497 tation with limited vocabulary extension, a combination of MSE loss, the standard AIM objective,
 498 and frozen original embeddings is optimal. For multilingual adaptation, unfreezing the original em-
 499 beddings is preferable to accommodate broader semantic shifts. The AIM* variant offers a good
 500 compromise, reducing memory and runtime while only slightly lowering accuracy. Further VRAM
 501 savings are possible with a custom kernel for AIM computation.
 502

503 Finally, we observe a disparity in robustness relative to model size. Larger models appear more
 504 resilient to embedding initialization shocks. This is illustrated by the FOCUS initialization results
 505 on English: while Gemma 3 4B PT maintains high stability, Qwen3 0.6B suffers a notable perfor-
 506 mance drop even when only a few new tokens are introduced. This suggests that larger parameter
 507 counts may provide a buffer against the perturbations introduced during tokenizer transfer. How-
 508 ever, this behavior may also be intrinsic to the specific model families, and thus requires further
 509 experimentation.
 510

5 CONCLUSION

511 In this work, we introduced MATT, a model-aware method for tokenizer transfer that leverages the
 512 internal dynamics of LLMs. We applied MATT to extend the tokenizers of Gemma 3 and Qwen
 513 3 models across multiple languages and settings, demonstrating that it consistently recovers a large
 514 portion of the original model’s capabilities while requiring only a few GPU hours of training. Unlike
 515 heuristic-based methods that rely solely on the embedding layer, MATT refines token representa-
 516 tions with direct feedback from the model, thanks to the novel Attention Influence Modeling (AIM)
 517 objective, allowing it to bridge the performance gap caused by tokenizer changes more effectively.
 518

519 Our experiments highlight this advantage most clearly in the transfer of the 12 billion-parameter
 520 Gemma 3 model to Ukrainian. With the extended tokenizer introducing over 80,000 new tokens,
 521 MATT achieves an average score of 77.27 out of the original 78.18 on the discriminative tasks
 522 and 6.45 out of 8.13 on the generative ones, outperforming both heuristic and optimization-based
 523 baselines. This substantial improvement underscores the value of incorporating model dynamics into
 524 tokenizer transfer and shows that high performance can be retained at a fraction of the computational
 525 cost typically required for NTP training.
 526

LIMITATIONS

528 The first limitation lies in the fact that MATT relies on tied input and output embeddings to fully
 529 realize its advantages. We outline possible strategies to relax this requirement in the Appendix D.
 530

531 Second, we do not perform continual pretraining with all weights unfrozen due to computational
 532 constraints, and instead evaluate only models with initialized or trained embedding layers. This
 533 is sufficient to compare MATT with existing baselines, whose primary goal is to provide a strong
 534 starting point for further adaptation.
 535

536 A further limitation is the need for an additional forward pass during optimization through the model
 537 using the original tokenizer to obtain targets for the AIM objective. Although this adds computa-
 538 tional overhead, the cost remains lower than a full forward pass through the entire model, as the
 539 target layer is positioned roughly one-third of the way through the network.
 540

Finally, we have not tested MATT on encoder-only architectures. In principle, applying it to such
 models would only require removing the causal constraint in the AIM definition.
 541

540 REFERENCES
541

542 Mehdi Ali, Michael Fromm, Klaudia Thellmann, Richard Rutmann, Max Lübbing, Johannes
543 Leveling, Katrin Klug, Jan Ebert, Niclas Doll, Jasper Buschhoff, Charvi Jain, Alexander We-
544 ber, Lena Jurkschat, Hammam Abdelwahab, Chelsea John, Pedro Ortiz Suarez, Malte Os-
545 tendorff, Samuel Weinbach, Rafet Sifa, Stefan Kesselheim, and Nicolas Flores-Herr. Tok-
546 enizer choice for LLM training: Negligible or crucial? In Kevin Duh, Helena Gomez, and
547 Steven Bethard (eds.), *Findings of the Association for Computational Linguistics: NAACL 2024*,
548 pp. 3907–3924, Mexico City, Mexico, June 2024. Association for Computational Linguistics.
549 doi: 10.18653/v1/2024.findings-naacl.247. URL [https://aclanthology.org/2024.
550 findings-naacl.247/](https://aclanthology.org/2024.findings-naacl.247/).

551 Loubna Ben Allal, Lewis Tunstall, Nouamane Tazi, Elie Bakouch, Ed Beeching, Carlos Miguel
552 Patiño, Clémentine Fourrier, Thibaud Frere, Anton Lozhkov, Colin Raffel, Leandro von Werra,
553 and Thomas Wolf. The smol training playbook: The secrets to building world-class llms, 2025.

554 Ebtesam Almazrouei, Hamza Alobeidli, Abdulaziz Alshamsi, Alessandro Cappelli, Ruxandra Co-
555 jocaru, Mérouane Debbah, Étienne Goffinet, Daniel Hesslow, Julien Launay, Quentin Malartic,
556 et al. The falcon series of open language models. *arXiv preprint arXiv:2311.16867*, 2023.

557 Mikel Artetxe, Sebastian Ruder, and Dani Yogatama. On the cross-lingual transferability of mono-
558 lingual representations. In Dan Jurafsky, Joyce Chai, Natalie Schluter, and Joel Tetreault (eds.),
559 *Proceedings of the 58th Annual Meeting of the Association for Computational Linguistics*, pp.
560 4623–4637, Online, July 2020. Association for Computational Linguistics. doi: 10.18653/v1/
561 2020.acl-main.421. URL <https://aclanthology.org/2020.acl-main.421/>.

562 Jinze Bai, Shuai Bai, Yunfei Chu, Zeyu Cui, Kai Dang, Xiaodong Deng, Yang Fan, Wenbin Ge,
563 Yu Han, Fei Huang, et al. Qwen technical report. *arXiv preprint arXiv:2309.16609*, 2023.

564 Lucas Bandarkar, Davis Liang, Benjamin Muller, Mikel Artetxe, Satya Narayan Shukla, Donald
565 Husa, Naman Goyal, Abhinandan Krishnan, Luke Zettlemoyer, and Madian Khabsa. The belebele
566 benchmark: a parallel reading comprehension dataset in 122 language variants. In Lun-Wei Ku,
567 Andre Martins, and Vivek Srikanth (eds.), *Proceedings of the 62nd Annual Meeting of the Association
568 for Computational Linguistics (Volume 1: Long Papers)*, pp. 749–775, Bangkok, Thailand,
569 August 2024. Association for Computational Linguistics. doi: 10.18653/v1/2024.acl-long.44.
570 URL <https://aclanthology.org/2024.acl-long.44/>.

571 Francesco Bertolotti and Walter Cazzola. By tying embeddings you are assuming the distributional
572 hypothesis. In *Forty-first International Conference on Machine Learning*, 2024. URL <https://openreview.net/forum?id=yyYMAprcAR>.

573 Terra Blevins and Luke Zettlemoyer. Language contamination helps explains the cross-lingual capa-
574 bilities of English pretrained models. In Yoav Goldberg, Zornitsa Kozareva, and Yue Zhang (eds.),
575 *Proceedings of the 2022 Conference on Empirical Methods in Natural Language Processing*, pp.
576 3563–3574, Abu Dhabi, United Arab Emirates, December 2022. Association for Computational
577 Linguistics. doi: 10.18653/v1/2022.emnlp-main.233. URL [https://aclanthology.org/2022.emnlp-main.233/](https://aclanthology.org/2022.emnlp-main.233).

578 Bohdan Didenko. Post #9194 on Telegram Channel Zaduha. <https://t.me/zaduha/9194>,
579 2025. [Online; accessed 26 June 2025].

580 Piotr Bojanowski, Edouard Grave, Armand Joulin, and Tomas Mikolov. Enriching word vectors with
581 subword information. *Transactions of the association for computational linguistics*, 5:135–146,
582 2017.

583 Laurie Burchell, Ona de Gibert, Nikolay Arefyev, Mikko Aulamo, Marta Bañón, Mariia Fedorova,
584 Liane Guillou, Barry Haddow, Jan Hajič, Erik Henriksson, et al. An expanded massive multi-
585 lingual dataset for high-performance language technologies. *arXiv preprint arXiv:2503.10267*,
586 2025.

587 Yihong Chen, Kelly Marchisio, Roberta Raileanu, David Adelani, Pontus Lars Erik Saito Stenetorp,
588 Sebastian Riedel, and Mikel Artetxe. Improving language plasticity via pretraining with active
589 forgetting. *Advances in Neural Information Processing Systems*, 36:31543–31557, 2023.

594 Alexis Conneau, Kartikay Khandelwal, Naman Goyal, Vishrav Chaudhary, Guillaume Wenzek,
 595 Francisco Guzmán, Edouard Grave, Myle Ott, Luke Zettlemoyer, and Veselin Stoyanov. Un-
 596 supervised cross-lingual representation learning at scale. In Dan Jurafsky, Joyce Chai, Natalie
 597 Schluter, and Joel Tetreault (eds.), *Proceedings of the 58th Annual Meeting of the Association
 598 for Computational Linguistics*, pp. 8440–8451, Online, July 2020. Association for Computational
 599 Linguistics. doi: 10.18653/v1/2020.acl-main.747. URL <https://aclanthology.org/2020.acl-main.747>.

600

601 Damai Dai, Li Dong, Yaru Hao, Zhifang Sui, Baobao Chang, and Furu Wei. Knowledge neurons
 602 in pretrained transformers. In Smaranda Muresan, Preslav Nakov, and Aline Villavicencio (eds.),
 603 *Proceedings of the 60th Annual Meeting of the Association for Computational Linguistics (Volume
 604 1: Long Papers)*, pp. 8493–8502, Dublin, Ireland, May 2022. Association for Computational
 605 Linguistics. doi: 10.18653/v1/2022.acl-long.581. URL [https://aclanthology.org/2022.acl-long.581/](https://aclanthology.org/2022.acl-long.581).

606

607 John Dang, Shivalika Singh, Daniel D’souza, Arash Ahmadian, Alejandro Salamanca, Made-
 608 line Smith, Aidan Peppin, Sungjin Hong, Manoj Govindassamy, Terrence Zhao, et al. Aya
 609 expanse: Combining research breakthroughs for a new multilingual frontier. *arXiv preprint
 610 arXiv:2412.04261*, 2024.

611

612 Wietse de Vries and Malvina Nissim. As good as new. how to successfully recycle english gpt-2 to
 613 make models for other languages. *arXiv preprint arXiv:2012.05628*, 2020.

614

615 Daniel Deutsch, Eleftheria Briakou, Isaac Caswell, Mara Finkelstein, Rebecca Galor, Juraj Juraska,
 616 Geza Kovacs, Alison Lui, Ricardo Rei, Jason Riesa, Shruti Rijhwani, Parker Riley, Elizabeth
 617 Salesky, Firas Trabelsi, Stephanie Winkler, Biao Zhang, and Markus Freitag. WMT24++: Ex-
 618 panding the Language Coverage of WMT24 to 55 Languages Dialects, 2025. URL <https://arxiv.org/abs/2502.12404>.

619

620 Konstantin Dobler and Gerard de Melo. FOCUS: Effective embedding initialization for mono-
 621 lingual specialization of multilingual models. In Houda Bouamor, Juan Pino, and Kalika Bali
 622 (eds.), *Proceedings of the 2023 Conference on Empirical Methods in Natural Language Pro-
 623 cessing*, pp. 13440–13454, Singapore, December 2023. Association for Computational Linguis-
 624 tics. doi: 10.18653/v1/2023.emnlp-main.829. URL [https://aclanthology.org/2023.emnlp-main.829/](https://aclanthology.org/2023.emnlp-main.829).

625

626 Konstantin Dobler, Desmond Elliott, and Gerard de Melo. Awedist: Attention-aware embedding
 627 distillation for new input token embeddings. *arXiv preprint arXiv:2505.20133*, 2025.

628

629 Chris Dyer, Victor Chahuneau, and Noah A Smith. A simple, fast, and effective reparameterization
 630 of ibm model 2. In *Proceedings of the 2013 conference of the North American chapter of the
 631 association for computational linguistics: human language technologies*, pp. 644–648, 2013.

632

633 Leo Gao, Jonathan Tow, Baber Abbasi, Stella Biderman, Sid Black, Anthony DiPofi, Charles Fos-
 634 ter, Laurence Golding, Jeffrey Hsu, Alain Le Noac’h, Haonan Li, Kyle McDonell, Niklas Muen-
 635 nighoff, Chris Ociepa, Jason Phang, Laria Reynolds, Hailey Schoelkopf, Aviya Skowron, Lintang
 636 Sutawika, Eric Tang, Anish Thite, Ben Wang, Kevin Wang, and Andy Zou. The language model
 637 evaluation harness, 07 2024. URL <https://zenodo.org/records/12608602>.

638

639 Mor Geva, Roei Schuster, Jonathan Berant, and Omer Levy. Transformer feed-forward layers are
 640 key-value memories, 2021. URL <https://arxiv.org/abs/2012.14913>.

641

642 Evangelia Gogoulou, Ariel Ekgren, Tim Isbister, and Magnus Sahlgren. Cross-lingual transfer of
 643 monolingual models. In Nicoletta Calzolari, Frédéric Béchet, Philippe Blache, Khalid Choukri,
 644 Christopher Cieri, Thierry Declerck, Sara Goggi, Hitoshi Isahara, Bente Maegaard, Joseph Mari-
 645 ani, Hélène Mazo, Jan Odijk, and Stelios Piperidis (eds.), *Proceedings of the Thirteenth Language
 646 Resources and Evaluation Conference*, pp. 948–955, Marseille, France, June 2022. European
 647 Language Resources Association. URL <https://aclanthology.org/2022.lrec-1.100/>.

648

649 Naman Goyal, Cynthia Gao, Vishrav Chaudhary, Peng-Jen Chen, Guillaume Wenzek, Da Ju, San-
 650 jana Krishnan, Marc’Aurelio Ranzato, Francisco Guzmán, and Angela Fan. The flores-101 eval-
 651 uation benchmark for low-resource and multilingual machine translation. 2021.

648 Aaron Grattafiori, Abhimanyu Dubey, Abhinav Jauhri, Abhinav Pandey, Abhishek Kadian, Ahmad
 649 Al-Dahle, Aiesha Letman, Akhil Mathur, Alan Schelten, Alex Vaughan, et al. The llama 3 herd
 650 of models. *arXiv preprint arXiv:2407.21783*, 2024.

651

652 Dirk Groeneveld, Iz Beltagy, Evan Walsh, Akshita Bhagia, Rodney Kinney, Oyvind Tafjord, Ananya
 653 Jha, Hamish Ivison, Ian Magnusson, Yizhong Wang, et al. Olmo: Accelerating the science of
 654 language models. In *Proceedings of the 62nd annual meeting of the association for computational
 655 linguistics (volume 1: Long papers)*, pp. 15789–15809, 2024.

656 Francisco Guzmán, Peng-Jen Chen, Myle Ott, Juan Pino, Guillaume Lample, Philipp Koehn,
 657 Vishrav Chaudhary, and Marc’Aurelio Ranzato. Two new evaluation datasets for low-resource
 658 machine translation: Nepali-english and sinhala-english. 2019.

659

660 Mykola Haltiuk and Aleksander Smywiński-Pohl. On the path to make Ukrainian a high-resource
 661 language. In Mariana Romanышин (ed.), *Proceedings of the Fourth Ukrainian Natural Language
 662 Processing Workshop (UNLP 2025)*, pp. 120–130, Vienna, Austria (online), July 2025. Associa-
 663 tion for Computational Linguistics. ISBN 979-8-89176-269-5. doi: 10.18653/v1/2025.unlp-1.14.
 664 URL <https://aclanthology.org/2025.unlp-1.14/>.

665

666 Tahmid Hasan, Abhik Bhattacharjee, Md. Saiful Islam, Kazi Mubasshir, Yuan-Fang Li, Yong-Bin
 667 Kang, M. Sohel Rahman, and Rifat Shahriyar. XL-sum: Large-scale multilingual abstractive
 668 summarization for 44 languages. In Chengqing Zong, Fei Xia, Wenjie Li, and Roberto Navigli
 669 (eds.), *Findings of the Association for Computational Linguistics: ACL-IJCNLP 2021*, pp. 4693–
 670 4703, Online, August 2021. Association for Computational Linguistics. doi: 10.18653/v1/2021.
 findings-acl.413. URL <https://aclanthology.org/2021.findings-acl.413/>.

671

672 Dan Hendrycks, Collin Burns, Steven Basart, Andy Zou, Mantas Mazeika, Dawn Song, and
 673 Jacob Steinhardt. Measuring massive multitask language understanding. *arXiv preprint
 674 arXiv:2009.03300*, 2020.

675

676 Sukjun Hwang, Brandon Wang, and Albert Gu. Dynamic chunking for end-to-end hierarchical
 677 sequence modeling. *arXiv preprint arXiv:2507.07955*, 2025.

678

679 Albert Q. Jiang, Alexandre Sablayrolles, Arthur Mensch, Chris Bamford, Devendra Singh Chap-
 680 lot, Diego de las Casas, Florian Bressand, Gianna Lengyel, Guillaume Lample, Lucile Saulnier,
 681 Lélio Renard Lavaud, Marie-Anne Lachaux, Pierre Stock, Teven Le Scao, Thibaut Lavril,
 Thomas Wang, Timothée Lacroix, and William El Sayed. Mistral 7b, 2023. URL <https://arxiv.org/abs/2310.06825>.

682

683 Guy Kaplan, Matanel Oren, Yuval Reif, and Roy Schwartz. From tokens to words: On the inner
 684 lexicon of llms. *arXiv preprint arXiv:2410.05864*, 2024.

685

686 Chong Li, Jiajun Zhang, and Chengqing Zong. TokAlign: Efficient vocabulary adaptation via to-
 687 ken alignment. In Wanxiang Che, Joyce Nabende, Ekaterina Shutova, and Mohammad Taher
 688 Pilehvar (eds.), *Proceedings of the 63rd Annual Meeting of the Association for Computational
 689 Linguistics (Volume 1: Long Papers)*, pp. 4109–4126, Vienna, Austria, July 2025. Association
 690 for Computational Linguistics. ISBN 979-8-89176-251-0. doi: 10.18653/v1/2025.acl-long.207.
 URL <https://aclanthology.org/2025.acl-long.207/>.

691

692 Davis Liang, Hila Gonen, Yuning Mao, Rui Hou, Naman Goyal, Marjan Ghazvininejad, Luke Zettle-
 693 moyer, and Madian Khabsa. XLM-V: Overcoming the vocabulary bottleneck in multilingual
 694 masked language models. In Houda Bouamor, Juan Pino, and Kalika Bali (eds.), *Proceedings of
 695 the 2023 Conference on Empirical Methods in Natural Language Processing*, pp. 13142–13152,
 696 Singapore, December 2023. Association for Computational Linguistics. doi: 10.18653/v1/2023.
 emnlp-main.813. URL <https://aclanthology.org/2023.emnlp-main.813/>.

697

698 Pierre Lison and Jörg Tiedemann. OpenSubtitles2016: Extracting large parallel corpora from movie
 699 and TV subtitles. In Nicoletta Calzolari, Khalid Choukri, Thierry Declerck, Sara Goggi, Marko
 700 Grobelnik, Bente Maegaard, Joseph Mariani, Helene Mazo, Asuncion Moreno, Jan Odijk, and
 Stelios Piperidis (eds.), *Proceedings of the Tenth International Conference on Language Re-
 701 sources and Evaluation (LREC’16)*, pp. 923–929, Portorož, Slovenia, May 2016. European Lan-
 guage Resources Association (ELRA). URL <https://aclanthology.org/L16-1147/>.

702 Yihong Liu, Peiqin Lin, Mingyang Wang, and Hinrich Schuetze. OFA: A framework of initializing
 703 unseen subword embeddings for efficient large-scale multilingual continued pretraining.
 704 In Kevin Duh, Helena Gomez, and Steven Bethard (eds.), *Findings of the Association for
 705 Computational Linguistics: NAACL 2024*, pp. 1067–1097, Mexico City, Mexico, June 2024.
 706 Association for Computational Linguistics. doi: 10.18653/v1/2024.findings-naacl.68. URL
 707 <https://aclanthology.org/2024.findings-naacl.68/>.

708 Ilya Loshchilov and Frank Hutter. Fixing weight decay regularization in adam. *CoRR*,
 709 abs/1711.05101, 2017. URL <http://arxiv.org/abs/1711.05101>.

710

711 Kelly Marchisio, Patrick Lewis, Yihong Chen, and Mikel Artetxe. Mini-model adaptation: Ef-
 712 ficiently extending pretrained models to new languages via aligned shallow training. In Anna
 713 Rogers, Jordan Boyd-Graber, and Naoaki Okazaki (eds.), *Findings of the Association for Com-
 714 putational Linguistics: ACL 2023*, pp. 5474–5490, Toronto, Canada, July 2023. Association
 715 for Computational Linguistics. doi: 10.18653/v1/2023.findings-acl.338. URL <https://aclanthology.org/2023.findings-acl.338/>.

716

717 Benjamin Minixhofer, Fabian Paischer, and Navid Rekabsaz. WECHSEL: Effective initializa-
 718 tion of subword embeddings for cross-lingual transfer of monolingual language models. In Marine
 719 Carpuat, Marie-Catherine de Marneffe, and Ivan Vladimir Meza Ruiz (eds.), *Proceed-
 720 ings of the 2022 Conference of the North American Chapter of the Association for Com-
 721 putational Linguistics: Human Language Technologies*, pp. 3992–4006, Seattle, United States, July
 722 2022. Association for Computational Linguistics. doi: 10.18653/v1/2022.naacl-main.293. URL
 723 <https://aclanthology.org/2022.naacl-main.293>.

724

725 Benjamin Minixhofer, Edoardo M. Ponti, and Ivan Vulić. Zero-shot tokenizer transfer. In A. Glober-
 726 son, L. Mackey, D. Belgrave, A. Fan, U. Paquet, J. Tomczak, and C. Zhang (eds.), *Advances in
 727 Neural Information Processing Systems*, volume 37, pp. 46791–46818. Curran Associates, Inc.,
 728 2024. URL https://proceedings.neurips.cc/paper_files/paper/2024/file/532ce4fcf853023c4cf2ac38cbc5d002-Paper-Conference.pdf.

729

730 Eshaan Nichani, Jason D. Lee, and Alberto Bietti. Understanding factual recall in transformers via
 731 associative memories, 2024. URL <https://arxiv.org/abs/2412.06538>.

732

733 James Cross Onur Çelebi Maha Elbayad Kenneth Heffernan Kevin Heffernan Elahe Kalbassi Jan-
 734 ice Lam Daniel Licht Jean Maillard Anna Sun Skyler Wang Guillaume Wenzek Al Youngblood
 735 Bapi Akula Loic Barrault Gabriel Mejia Gonzalez Prangthip Hansanti John Hoffman Semarley
 736 Jarrett Kaushik Ram Sadagopan Dirk Rowe Shannon Spruit Chau Tran Pierre Andrews Necip
 737 Fazil Ayan Shruti Bhosale Sergey Edunov Angela Fan Cynthia Gao Vedanuj Goswami Fran-
 738 cisco Guzmán Philipp Koehn Alexandre Mourachko Christophe Ropers Safiyyah Saleem Holger
 739 Schwenk Jeff Wang NLLB Team, Marta R. Costa-jussà. No language left behind: Scaling human-
 740 centered machine translation. 2022.

741

742 Krzysztof Ociepa, Krzysztof Wróbel, Adrian Gwoździej, Remigiusz Kinas, et al. Bielik
 743 7b v0. 1: A polish language model–development, insights, and evaluation. *arXiv preprint
 744 arXiv:2410.18565*, 2024.

745

746 Malte Ostendorff and Georg Rehm. Efficient language model training through cross-lingual and
 747 progressive transfer learning. *arXiv preprint arXiv:2301.09626*, 2023.

748

749 Enes Özeren, Yihong Liu, and Hinrich Schuetze. HYPEROFA: Expanding LLM vocabulary to new
 750 languages via hypernetwork-based embedding initialization. In Jin Zhao, Mingyang Wang, and
 751 Zhu Liu (eds.), *Proceedings of the 63rd Annual Meeting of the Association for Computational Lin-
 752 guistics (Volume 4: Student Research Workshop)*, pp. 79–96, Vienna, Austria, July 2025. Associa-
 753 tion for Computational Linguistics. ISBN 979-8-89176-254-1. doi: 10.18653/v1/2025.acl-srw.6.
 754 URL <https://aclanthology.org/2025.acl-srw.6/>.

755

756 Artidoro Pagnoni, Ramakanth Pasunuru, Pedro Rodriguez, John Nguyen, Benjamin Muller, Mar-
 757 garet Li, Chunting Zhou, Lili Yu, Jason E Weston, Luke Zettlemoyer, Gargi Ghosh, Mike
 758 Lewis, Ari Holtzman, and Srini Iyer. Byte latent transformer: Patches scale better than to-
 759 kens. In Wanxiang Che, Joyce Nabende, Ekaterina Shutova, and Mohammad Taher Pilehvar
 760 (eds.), *Proceedings of the 63rd Annual Meeting of the Association for Computational Linguistics*

756 (Volume 1: Long Papers), pp. 9238–9258, Vienna, Austria, July 2025. Association for Com-
 757 putational Linguistics. ISBN 979-8-89176-251-0. doi: 10.18653/v1/2025.acl-long.453. URL
 758 <https://aclanthology.org/2025.acl-long.453/>.

759

760 Yurii Paniv. Isolating llm performance gains in pre-training versus instruction-tuning for mid-
 761 resource languages: The ukrainian benchmark study. In *Proceedings of the 15th International*
 762 *Conference on Recent Advances in Natural Language Processing - Natural Language Process-*
 763 *ing in the Generative AI era*, pp. 876–883, Varna, Bulgaria, September 2025. INCOMA Ltd.,
 764 Shoumen, Bulgaria. URL <https://aclanthology.org/2025.ranlp-1.100>.

765

766 Jeffrey Pennington, Richard Socher, and Christopher Manning. GloVe: Global vectors for word
 767 representation. In Alessandro Moschitti, Bo Pang, and Walter Daelemans (eds.), *Proceedings*
 768 *of the 2014 Conference on Empirical Methods in Natural Language Processing (EMNLP)*, pp.
 769 1532–1543, Doha, Qatar, October 2014. Association for Computational Linguistics. doi: 10.
 3115/v1/D14-1162. URL <https://aclanthology.org/D14-1162/>.

770

771 François Remy, Pieter Delobelle, Bettina Berendt, Kris Demuynck, and Thomas Demeester. Tik-to-
 772 tok: Translating language models one token at a time: An embedding initialization strategy for
 773 efficient language adaptation. *arXiv preprint arXiv:2310.03477*, 2023.

774

775 François Remy, Pieter Delobelle, Hayastan Avetisyan, Alfiya Khabibullina, Miryam de Lhoneux,
 776 and Thomas Demeester. Trans-tokenization and cross-lingual vocabulary transfers: Language
 777 adaptation of llms for low-resource nlp. *arXiv preprint arXiv:2408.04303*, 2024.

778

779 Piotr Rybak. Maupqa: Massive automatically-created polish question answering dataset. *arXiv*
 780 preprint [arXiv:2305.05486](https://arxiv.org/abs/2305.05486), 2023.

781

782 Shivalika Singh, Angelika Romanou, Clémentine Fourrier, David Ifeoluwa Adelani, Jian Gang
 783 Ngui, Daniel Vila-Suero, Peerat Limkonchotiwat, Kelly Marchisio, Wei Qi Leong, Yosephine
 784 Susanto, Raymond Ng, Shayne Longpre, Sebastian Ruder, Wei-Yin Ko, Antoine Bosselut, Alice
 785 Oh, Andre Martins, Leshem Choshen, Daphne Ippolito, Enzo Ferrante, Marzieh Fadaee, Beyza
 786 Ermis, and Sara Hooker. Global MMLU: Understanding and addressing cultural and linguistic
 787 biases in multilingual evaluation. In Wanxiang Che, Joyce Nabende, Ekaterina Shutova, and Mo-
 788 hammad Taher Pilehvar (eds.), *Proceedings of the 63rd Annual Meeting of the Association for*
 789 *Computational Linguistics (Volume 1: Long Papers)*, pp. 18761–18799, Vienna, Austria, July
 2025. Association for Computational Linguistics. ISBN 979-8-89176-251-0. doi: 10.18653/v1/
 2025.acl-long.919. URL <https://aclanthology.org/2025.acl-long.919/>.

790

791 Sho Takase, Ryokan Ri, Shun Kiyono, and Takuya Kato. Large vocabulary size improves large
 792 language models. In Wanxiang Che, Joyce Nabende, Ekaterina Shutova, and Mohammad Taher
 793 Pilehvar (eds.), *Findings of the Association for Computational Linguistics: ACL 2025*, pp. 1015–
 794 1026, Vienna, Austria, July 2025. Association for Computational Linguistics. ISBN 979-8-
 795 89176-256-5. doi: 10.18653/v1/2025.findings-acl.57. URL [https://aclanthology.org/2025.findings-acl.57/](https://aclanthology.org/2025.findings-acl.57).

796

797 S. Tamang and D. J. Bora. Evaluating tokenizer performance of large language models across official
 798 indian languages, 2024. URL <https://arxiv.org/abs/2411.12240>.

799

800 Gemma Team, Thomas Mesnard, Cassidy Hardin, Robert Dadashi, Surya Bhupatiraju, Shreya
 801 Pathak, Laurent Sifre, Morgane Rivière, Mihir Sanjay Kale, Juliette Love, et al. Gemma: Open
 802 models based on gemini research and technology. *arXiv preprint arXiv:2403.08295*, 2024a.

803

804 Gemma Team, Morgane Riviere, Shreya Pathak, Pier Giuseppe Sessa, Cassidy Hardin, Surya Bhu-
 805 patiraju, Léonard Hussonot, Thomas Mesnard, Bobak Shahriari, Alexandre Ramé, et al. Gemma 2: Im-
 806 proving open language models at a practical size. *arXiv preprint arXiv:2408.00118*, 2024b.

807

808 Gemma Team, Aishwarya Kamath, Johan Ferret, Shreya Pathak, Nino Vieillard, Ramona Merhej,
 809 Sarah Perrin, Tatiana Matejovicova, Alexandre Ramé, Morgane Rivière, et al. Gemma 3 technical
 810 report. *arXiv preprint arXiv:2503.19786*, 2025.

811

Qwen Team. Qwen3 technical report, 2025. URL <https://arxiv.org/abs/2505.09388>.

810 Hugo Touvron, Thibaut Lavril, Gautier Izacard, Xavier Martinet, Marie-Anne Lachaux, Timothée
 811 Lacroix, Baptiste Rozière, Naman Goyal, Eric Hambro, Faisal Azhar, et al. Llama: Open and
 812 efficient foundation language models. *arXiv preprint arXiv:2302.13971*, 2023.
 813
 814
 815
 816
 817
 818
 819
 820
 821
 822
 823
 824
 825
 826

A SEGMENTATION ALGORITHM

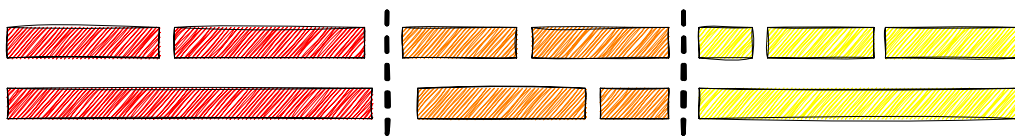
833 Instead of relying on word-based segmentation, we use an offset-based segmentation strategy. De-
 834 signing a consistent word segmentation across tokenizers is challenging because tokenizers often
 835 differ in normalization rules, pre-tokenization steps, language coverage, etc. These differences make
 836 it difficult to ensure that segment boundaries match at the word level.

837 The offset-based method addresses this by operating directly on character offsets in the original text.
 838 Given two different tokenizations of the same string, along with the start and end positions of each
 839 token, the algorithm searches for all possible split positions that never cut through the middle of any
 840 token (see Figure 3).

841 This approach is universal: such a segmentation always exists, even if the worst case reduces to a
 842 single segment spanning the entire input. It can also lead to more precise alignments because the
 843 target tokenizer may break a word into several sub-tokens. By working with character offsets, we
 844 can introduce mid-word segment boundaries whenever they yield a better match.

845 For example, consider the sentence *CH4 is a formula for methane*. Suppose the original tokenizer
 846 produces the tokens `_for`, `m`, and `ula` for the word *formula*, while the new tokenizer produces
 847 `_form` and `ula`. A word-level strategy would force alignment at the whole-word boundary, but an
 848 offset-based method can instead match `_for` and `m` with `_form`, and `ula` with `ula`, which more
 849 closely respects both tokenizations.

850 Algorithm 1 provides detailed pseudocode for implementation.
 851
 852
 853
 854
 855
 856
 857
 858



859
 860
 861
 862
 863 Figure 3: Offset-based segmentation algorithm visualization.

864 **Algorithm 1:** Offset–Based Segmentation

865 **Input:** teacher offsets O_t , student offsets O_s

866 **Output:** teacher segment ids S_t , student segment ids S_s

867 ▷ *initialize outputs and counters*

868 1 $S_t \leftarrow []$, $S_s \leftarrow []$

869 2 $e \leftarrow -1$; ▷ *current end*

870 3 $k \leftarrow -1$; ▷ *current segment id*

871 ▷ *iterate until both queues empty*

872 4 **while** $O_t \neq \emptyset$ **or** $O_s \neq \emptyset$ **do**

873 ▷ *if one side empty, label all remaining tokens with current segment id*

874 5 **if** $O_t = \emptyset$ **then**

875 6 **for** *each* o *in* O_s **do**

876 7 append k to S_s

877 8 **break**

878 9 **else if** $O_s = \emptyset$ **then**

879 10 **for** *each* o *in* O_t **do**

880 11 append k to S_t

881 12 **break**

882 ▷ *peek next offsets*

883 13 $(t_s, t_e) \leftarrow \text{peek}(O_t)$, $(s_s, s_e) \leftarrow \text{peek}(O_s)$

884 ▷ *continue with the same segment if overlap*

885 14 **if** $t_s < e$ **then**

886 15 append k to S_t , $\text{pop}(O_t)$

887 16 $e \leftarrow \max(e, t_e)$

888 17 **else if** $s_s < e$ **then**

889 18 append k to S_s , $\text{pop}(O_s)$

890 19 $e \leftarrow \max(e, s_e)$

891 ▷ *else start a new segment*

892 20 **else**

893 21 $k \leftarrow k + 1$

894 22 append k to S_t and S_s , $\text{pop}(O_t)$, $\text{pop}(O_s)$

895 23 $e \leftarrow \max(t_e, s_e)$

896 24 **return** (S_t, S_s)

903

904

B CONVERGENCE SPEED

907 We repeated the experiment with Gemma 3 4B PT described in Section 4.2, but this time we saved
 908 model checkpoints every 3,000 training steps. While the results in Table 3 were obtained after
 909 250,000 steps, this setup allows us to observe how quickly the embeddings adapt to the new tokenizer
 910 and to evaluate whether training can be substantially shortened.

911 The AIM objective provides a rich learning signal for tuning the embeddings. Using a mean squared
 912 error (MSE) loss, the number of value pairs contributing to the objective is proportional to the
 913 product of the head dimensionality, the number of attention heads, the number of possible segment
 914 pairs, and the batch size. In the configuration used here – four documents per batch, each truncated
 915 to 256 tokens – this amounts to hundreds of millions of pairs at every step of the training.

916 Table 4 presents the results for the first eight checkpoints on the Belebele benchmark across all
 917 tested languages, while Figure 4 provides a visual view of the same trends.

918
 919
 920
 921
 922
 923
 The data show that more than 50% of the final performance gains can be achieved in under 10% of
 924
 925
 926
 927
 928
 929
 930
 931
 932
 933
 934
 935
 936
 937
 938
 939
 940
 941
 942
 943
 944
 945
 946
 947
 948
 949
 950
 951
 952
 953
 954
 955
 956
 957
 958
 959
 960
 961
 962
 963
 964
 965
 966
 967
 968
 969
 970
 971
 972
 973
 974
 975
 976
 977
 978
 979
 980
 981
 982
 983
 984
 985
 986
 987
 988
 989
 990
 991
 992
 993
 994
 995
 996
 997
 998
 999
 1000
 1001
 1002
 1003
 1004
 1005
 1006
 1007
 1008
 1009
 1010
 1011
 1012
 1013
 1014
 1015
 1016
 1017
 1018
 1019
 1020
 1021
 1022
 1023
 1024
 1025
 1026
 1027
 1028
 1029
 1030
 1031
 1032
 1033
 1034
 1035
 1036
 1037
 1038
 1039
 1040
 1041
 1042
 1043
 1044
 1045
 1046
 1047
 1048
 1049
 1050
 1051
 1052
 1053
 1054
 1055
 1056
 1057
 1058
 1059
 1060
 1061
 1062
 1063
 1064
 1065
 1066
 1067
 1068
 1069
 1070
 1071
 1072
 1073
 1074
 1075
 1076
 1077
 1078
 1079
 1080
 1081
 1082
 1083
 1084
 1085
 1086
 1087
 1088
 1089
 1090
 1091
 1092
 1093
 1094
 1095
 1096
 1097
 1098
 1099
 1100
 1101
 1102
 1103
 1104
 1105
 1106
 1107
 1108
 1109
 1110
 1111
 1112
 1113
 1114
 1115
 1116
 1117
 1118
 1119
 1120
 1121
 1122
 1123
 1124
 1125
 1126
 1127
 1128
 1129
 1130
 1131
 1132
 1133
 1134
 1135
 1136
 1137
 1138
 1139
 1140
 1141
 1142
 1143
 1144
 1145
 1146
 1147
 1148
 1149
 1150
 1151
 1152
 1153
 1154
 1155
 1156
 1157
 1158
 1159
 1160
 1161
 1162
 1163
 1164
 1165
 1166
 1167
 1168
 1169
 1170
 1171
 1172
 1173
 1174
 1175
 1176
 1177
 1178
 1179
 1180
 1181
 1182
 1183
 1184
 1185
 1186
 1187
 1188
 1189
 1190
 1191
 1192
 1193
 1194
 1195
 1196
 1197
 1198
 1199
 1200
 1201
 1202
 1203
 1204
 1205
 1206
 1207
 1208
 1209
 1210
 1211
 1212
 1213
 1214
 1215
 1216
 1217
 1218
 1219
 1220
 1221
 1222
 1223
 1224
 1225
 1226
 1227
 1228
 1229
 1230
 1231
 1232
 1233
 1234
 1235
 1236
 1237
 1238
 1239
 1240
 1241
 1242
 1243
 1244
 1245
 1246
 1247
 1248
 1249
 1250
 1251
 1252
 1253
 1254
 1255
 1256
 1257
 1258
 1259
 1260
 1261
 1262
 1263
 1264
 1265
 1266
 1267
 1268
 1269
 1270
 1271
 1272
 1273
 1274
 1275
 1276
 1277
 1278
 1279
 1280
 1281
 1282
 1283
 1284
 1285
 1286
 1287
 1288
 1289
 1290
 1291
 1292
 1293
 1294
 1295
 1296
 1297
 1298
 1299
 1300
 1301
 1302
 1303
 1304
 1305
 1306
 1307
 1308
 1309
 1310
 1311
 1312
 1313
 1314
 1315
 1316
 1317
 1318
 1319
 1320
 1321
 1322
 1323
 1324
 1325
 1326
 1327
 1328
 1329
 1330
 1331
 1332
 1333
 1334
 1335
 1336
 1337
 1338
 1339
 1340
 1341
 1342
 1343
 1344
 1345
 1346
 1347
 1348
 1349
 1350
 1351
 1352
 1353
 1354
 1355
 1356
 1357
 1358
 1359
 1360
 1361
 1362
 1363
 1364
 1365
 1366
 1367
 1368
 1369
 1370
 1371
 1372
 1373
 1374
 1375
 1376
 1377
 1378
 1379
 1380
 1381
 1382
 1383
 1384
 1385
 1386
 1387
 1388
 1389
 1390
 1391
 1392
 1393
 1394
 1395
 1396
 1397
 1398
 1399
 1400
 1401
 1402
 1403
 1404
 1405
 1406
 1407
 1408
 1409
 1410
 1411
 1412
 1413
 1414
 1415
 1416
 1417
 1418
 1419
 1420
 1421
 1422
 1423
 1424
 1425
 1426
 1427
 1428
 1429
 1430
 1431
 1432
 1433
 1434
 1435
 1436
 1437
 1438
 1439
 1440
 1441
 1442
 1443
 1444
 1445
 1446
 1447
 1448
 1449
 1450
 1451
 1452
 1453
 1454
 1455
 1456
 1457
 1458
 1459
 1460
 1461
 1462
 1463
 1464
 1465
 1466
 1467
 1468
 1469
 1470
 1471
 1472
 1473
 1474
 1475
 1476
 1477
 1478
 1479
 1480
 1481
 1482
 1483
 1484
 1485
 1486
 1487
 1488
 1489
 1490
 1491
 1492
 1493
 1494
 1495
 1496
 1497
 1498
 1499
 1500
 1501
 1502
 1503
 1504
 1505
 1506
 1507
 1508
 1509
 1510
 1511
 1512
 1513
 1514
 1515
 1516
 1517
 1518
 1519
 1520
 1521
 1522
 1523
 1524
 1525
 1526
 1527
 1528
 1529
 1530
 1531
 1532
 1533
 1534
 1535
 1536
 1537
 1538
 1539
 1540
 1541
 1542
 1543
 1544
 1545
 1546
 1547
 1548
 1549
 1550
 1551
 1552
 1553
 1554
 1555
 1556
 1557
 1558
 1559
 1560
 1561
 1562
 1563
 1564
 1565
 1566
 1567
 1568
 1569
 1570
 1571
 1572
 1573
 1574
 1575
 1576
 1577
 1578
 1579
 1580
 1581
 1582
 1583
 1584
 1585
 1586
 1587
 1588
 1589
 1590
 1591
 1592
 1593
 1594
 1595
 1596
 1597
 1598
 1599
 1600
 1601
 1602
 1603
 1604
 1605
 1606
 1607
 1608
 1609
 1610
 1611
 1612
 1613
 1614
 1615
 1616
 1617
 1618
 1619
 1620
 1621
 1622
 1623
 1624
 1625
 1626
 1627
 1628
 1629
 1630
 1631
 1632
 1633
 1634
 1635
 1636
 1637
 1638
 1639
 1640
 1641
 1642
 1643
 1644
 1645
 1646
 1647
 1648
 1649
 1650
 1651
 1652
 1653
 1654
 1655
 1656
 1657
 1658
 1659
 1660
 1661
 1662
 1663
 1664
 1665
 1666
 1667
 1668
 1669
 1670
 1671
 1672
 1673
 1674
 1675
 1676
 1677
 1678
 1679
 1680
 1681
 1682
 1683
 1684
 1685
 1686
 1687
 1688
 1689
 1690
 1691
 1692
 1693
 1694
 1695
 1696
 1697
 1698
 1699
 1700
 1701
 1702
 1703
 1704
 1705
 1706
 1707
 1708
 1709
 1710
 1711
 1712
 1713
 1714
 1715
 1716
 1717
 1718
 1719
 1720
 1721
 1722
 1723
 1724
 1725
 1726
 1727
 1728
 1729
 1730
 1731
 1732
 1733
 1734
 1735
 1736
 1737
 1738
 1739
 1740
 1741
 1742
 1743
 1744
 1745
 1746
 1747
 1748
 1749
 1750
 1751
 1752
 1753
 1754
 1755
 1756
 1757
 1758
 1759
 1760
 1761
 1762
 1763
 1764
 1765
 1766
 1767
 1768
 1769
 1770
 1771
 1772
 1773
 1774
 1775
 1776
 1777
 1778
 1779
 1780
 1781
 1782
 1783
 1784
 1785
 1786
 1787
 1788
 1789
 1790
 1791
 1792
 1793
 1794
 1795
 1796
 1797
 1798
 1799
 1800
 1801
 1802
 1803
 1804
 1805
 1806
 1807
 1808
 1809
 1810
 1811
 1812
 1813
 1814
 1815
 1816
 1817
 1818
 1819
 1820
 1821
 1822
 1823
 1824
 1825
 1826
 1827
 1828
 1829
 1830
 1831
 1832
 1833
 1834
 1835
 1836
 1837
 1838
 1839
 1840
 1841
 1842
 1843
 1844
 1845
 1846
 1847
 1848
 1849
 1850
 1851
 1852
 1853
 1854
 1855
 1856
 1857
 1858
 1859
 1860
 1861
 1862
 1863
 1864
 1865
 1866
 1867
 1868
 1869
 1870
 1871
 1872
 1873
 1874
 1875
 1876
 1877
 1878
 1879
 1880
 1881
 1882
 1883
 1884
 1885
 1886
 1887
 1888
 1889
 1890
 1891
 1892
 1893
 1894
 1895
 1896
 1897
 1898
 1899
 1900
 1901
 1902
 1903
 1904
 1905
 1906
 1907
 1908
 1909
 1910
 1911
 1912
 1913
 1914
 1915
 1916
 1917
 1918
 1919
 1920
 1921
 1922
 1923
 1924
 1925
 1926
 1927
 1928
 1929
 1930
 1931
 1932
 1933
 1934
 1935
 1936
 1937
 1938
 1939
 1940
 1941
 1942
 1943
 1944
 1945
 1946
 1947
 1948
 1949
 1950
 1951
 1952
 1953
 1954
 1955
 1956
 1957
 1958
 1959
 1960
 1961
 1962
 1963
 1964
 1965
 1966
 1967
 1968
 1969
 1970
 1971
 1972
 1973
 1974
 1975
 1976
 1977
 1978
 1979
 1980
 1981
 1982
 1983
 1984
 1985
 1986
 1987
 1988
 1989
 1990
 1991
 1992
 1993
 1994
 1995
 1996
 1997
 1998
 1999
 2000
 2001
 2002
 2003
 2004
 2005
 2006
 2007
 2008
 2009
 2010
 2011
 2012
 2013
 2014
 2015
 2016
 2017
 2018
 2019
 2020
 2021
 2022
 2023
 2024
 2025
 2026
 2027
 2028
 2029
 2030
 2031
 2032
 2033
 2034
 2035
 2036
 2037
 2038
 2039
 2040
 2041
 2042
 2043
 2044
 2045
 2046
 2047
 2048
 2049
 2050
 2051
 2052
 2053
 2054
 2055
 2056
 2057
 2058
 2059
 2060
 2061
 2062
 2063
 2064
 2065
 2066
 2067
 2068
 2069
 2070
 2071
 2072
 2073
 2074
 2075
 2076
 2077
 2078
 2079
 2080
 2081
 2082
 2083
 2084
 2085
 2086
 2087
 2088
 2089
 2090
 2091
 2092
 2093
 2094
 2095
 2096
 2097
 2098
 2099
 2100
 2101
 2102
 2103
 2104
 2105
 2106
 2107
 2108
 2109
 2110
 2111
 2112
 2113
 2114
 2115
 2116
 2117
 2118
 2119
 2120
 2121
 2122
 2123
 2124
 2125
 2126
 2127
 2128
 2129
 2130
 2131
 2132
 2133
 2134
 2135
 2136
 2137
 2138
 2139
 2140
 2141
 2142
 2143
 2144
 2145
 2146
 2147
 2148
 2149
 2150
 2151
 2152
 2153
 2154
 2155
 2156
 2157
 2158
 2159
 2160
 2161
 2162
 2163
 2164
 2165
 2166
 2167
 2168
 2169
 2170
 2171
 2172
 2173
 2174
 2175
 2176
 2177
 2178
 2179
 2180
 2181
 2182
 2183
 2184
 2185
 2186
 2187
 2188
 2189
 2190
 2191
 2192
 2193
 2194
 2195
 2196
 2197
 2198
 2199
 2200
 2201
 2202
 2203
 2204
 2205
 2206
 2207
 2208
 2209
 2210
 2211
 2212
 2213
 2214
 2215
 2216
 2217
 2218
 2219
 2220
 2221
 2222
 2223
 2224
 2225
 2226
 2227
 2228
 2229
 2230
 2231
 2232
 2233
 2234
 2235
 2236
 2237
 2238
 2239
 2240
 2241
 2242
 2243
 2244
 2245
 2246
 2247
 2248
 2249
 2250
 2251
 2252
 2253
 2254
 2255
 2256
 2257
 2258
 2259
 2260
 2261
 2262
 2263
 2264
 2265
 2266
 2267
 2268
 2269
 2270
 2271
 2272
 2273
 2274
 2275
 2276
 2277
 2278
 2279
 2280
 2281
 2282
 2283
 2284
 2285
 2286
 2287
 2288
 2289
 2290
 2291
 2292
 2293
 2294
 2295
 2296
 2297
 2298
 2299
 2300
 2301
 2302
 2303
 2304
 2305
 2306
 2307
 2308
 2309
 2310
 2311
 2312
 2313
 2314
 2315
 2316
 2317
 2318
 2319
 2320
 2321
 2322
 2323
 2324
 2325
 2326
 2327
 2328
 2329
 2330
 2331
 2332
 2333
 2334
 2335
 2336
 2337
 2338
 2339

972
 973 Table 4: Performance on the Belebele benchmark during early training of Gemma 3 4B PT with
 974 Model-Aware Tokenizer Transfer, showing rapid gains within the first 10% of steps compared to the
 975 full run.

976 977 978 979 980 981 982 983 984 985 986 987 988 989	990 991 992 993 994 995 996 997 998 999 1000 1001 1002 1003 1004 1005 1006 1007 1008 1009 1010 1011 1012 1013 1014 1015 1016 1017 1018 1019 1020 1021 1022 1023 1024 1025	991 992 993 994 995 996 997 998 999 1000 1001 1002 1003 1004 1005 1006 1007 1008 1009 1010 1011 1012 1013 1014 1015 1016 1017 1018 1019 1020 1021 1022 1023 1024 1025	Belebele						
			Steps #	Tokens #	ar	de	en	ja	sw
0k	0M	32.89	52.44	80.33	42.00	25.56			
3k	3M	34.78	56.89	80.33	45.33	30.33			
6k	6M	36.44	59.22	80.44	48.00	36.44			
9k	9M	37.00	63.44	80.44	50.56	37.67			
12k	12M	40.78	64.56	80.44	49.11	40.56			
15k	15M	42.56	65.56	80.44	48.11	42.00			
18k	18M	44.22	67.00	80.44	49.11	42.22			
21k	21M	45.89	67.56	80.56	49.67	43.22			
24k	24M	48.00	68.89	80.56	49.67	44.33			
250k	250M	62.44	72.56	80.67	58.00	54.67			

990
 991 Table 5: Ablation studies of MATT configurations. **3** and **5** denote the number of layers used for
 992 AIM objective.

	991 992 993 994 995 996 997 998 999 1000 1001 1002 1003 1004 1005 1006 1007 1008 1009 1010 1011 1012 1013 1014 1015 1016 1017 1018 1019 1020 1021 1022 1023 1024 1025	991 992 993 994 995 996 997 998 999 1000 1001 1002 1003 1004 1005 1006 1007 1008 1009 1010 1011 1012 1013 1014 1015 1016 1017 1018 1019 1020 1021 1022 1023 1024 1025	VRAM (GiB)		Time		Belebele		Global MMLU	
		3	5	3	5	3	5	3	5	
All Layers vs. Last Layer										
all layers	17.3	26.5	1h 33m	2h 19m	32.56	35.11	28.63	29.00		
last layer	9.1	10.1	0h 56m	1h 04m	37.22	60.11	29.95	34.80		
Initialization Method										
WECHSEL	9.1	10.1	0h 52m	1h 04m	42.22	59.78	29.82	33.56		
FOCUS	9.1	10.1	0h 55m	1h 06m	37.11	60.89	30.10	34.72		
Transtokenizers	9.1	10.1	0h 55m	1h 04m	52.44	60.89	32.43	34.75		

1006
 1007 **FOCUS and Transtokenizers perform similarly on higher layers, while WECHSEL underper-**
 1008 **forms.** Because MATT is independent of the embedding initialization method, different starting
 1009 points can be tested. We compare WECHSEL, FOCUS, and Transtokenizers. FOCUS and Transto-
 1010 kenizers perform similarly on higher layers, while WECHSEL lags behind (see Table 5). Although
 1011 Transtokenizers occasionally achieves the best scores, in other experiments, we find FOCUS to be
 1012 more stable across models, and therefore make it our default choice.

1013 Transtokenizers method may have an upper hand due to its better utilization of English embeddings,
 1014 as it learns an English-Ukrainian token-level dictionary from parallel corpora and utilizes it to trans-
 1015 fer embeddings from English tokens to their Ukrainian counterparts. Whereas FOCUS utilizes the
 1016 tokens' overlap to train a FastText model over it, and although it contains English tokens as well,
 1017 the FastText training corpus contains little data that encompasses both English and Ukrainian text
 1018 in the same document. This could potentially limit the FOCUS to pay attention mostly to Ukrainian
 1019 overlapped tokens, given the limited usability of English tokens' embeddings.

1020 MATT, in the way it uses existing embeddings, is conceptually closer to FOCUS than Transtokenizers,
 1021 as it models inter-token communication of original tokens, focusing predominantly on Ukrainian
 1022 ones. As denoted in Appendix B, MATT quickly converges, requiring little data to recover a large
 1023 part of the original model's performance. This means that small differences in the initialization
 1024 (the difference between average scores for FOCUS and Transtokenizers is less than 10% in the
 1025 case of Gemma 3 12B PT; see Table 1) are evened out during training. This can also be seen with
 WECHSEL, which performs considerably worse compared to FOCUS or Transtokenizers (Table 1),
 but achieves only slightly worse results after a round of MATT training, especially on higher lay-

1026
 1027
 1028
 1029
 1030
 1031
 1032
 1033
 1034
 1035
 1036
 1037
 1038
 1039
 1040
 1041
 1042
 1043
 1044
 1045
 1046
 1047
 1048
 1049
 1050
 1051
 1052
 1053
 1054
 1055
 1056
 1057
 1058
 1059
 1060
 1061
 1062
 1063
 1064
 1065
 1066
 1067
 1068
 1069
 1070
 1071
 1072
 1073
 1074
 1075
 1076
 1077
 1078
 1079
 ers (see Table 5). The final observation is presented in Table 1, where we see that even the NTP baseline starting from the Transtokenizers initialization, which is initially better, achieves similar performance to the NTP over FOCUS.

Minor efficiency differences in Table 5 are likely due to external factors such as checkpointing overhead.

AIM on higher layers leads to better results, but saturates at around one third of the model’s depth. MATT allows selecting how deep into the model the AIM objective is applied, creating a natural trade-off between efficiency and accuracy. We evaluate different target depths and find that performance steadily improves as AIM is applied to higher layers (see Figure 5), but gains saturate once the objective reaches roughly one third of the model’s total depth. In contrast, memory consumption and training time continue to grow almost linearly with the number of layers, highlighting the cost of deeper alignment.

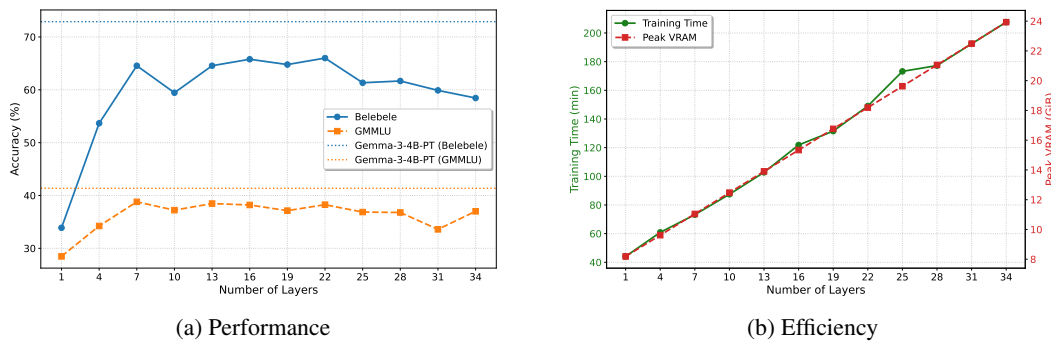


Figure 5: Effect of applying the AIM objective to different numbers of layers. The plots show the trade-off between model performance (a) and computational efficiency (b) as the application depth increases.

D ADDRESSING THE TIED EMBEDDINGS REQUIREMENT

The use of tied embeddings varies greatly both between the model families and model sizes. For example, Llama 3.2 1B and Llama 3.2 3B (Grattafiori et al., 2024) both utilize tied embeddings to reduce the number of parameters, whereas a larger Llama 3.1 8B does not. In contrast, the Gemma family (Team et al., 2024a;b; 2025) consistently uses tied embeddings across all sizes.

A significant amount of model pretraining research conducts very little to no experimentation on the effects of embedding tying (Jiang et al., 2023; Touvron et al., 2023; Groeneveld et al., 2024; Team, 2025). And those that do (Bai et al., 2023) offer a limited explanation of the reasons behind their choice, referring to preliminary results that are not reported in the paper.

More recent research suggests that embedding tying is more effective both from a theoretical standpoint (Bertolotti & Cazzola, 2024) and in achieving lower validation loss and better performance on downstream tasks (Allal et al., 2025). This leads us to believe that the share of models with tied embeddings may increase in the coming years, making our method even more relevant.

We conducted additional experiments on Mistral 7B v0.1 (Jiang et al., 2023), which does not tie embeddings. The results are presented in Table 6. The original Mistral’s tokenizer has a vocabulary size of 32,000 and achieves a compression rate of 2.24 on Ukrainian data. We transfer Mistral to an extended vocabulary comprising over 177k tokens (a 5.5x increase, with a 4.10 compression rate). We compare the original model’s performance to the FOCUS initialization, NTP optimization over both input and output embeddings, MATT with different compute budgets, and MATT combined with further NTP optimization, where we first train input embeddings using MATT, and then train only output embeddings using the NTP objective to match the budget of the NTP baseline.

MATT is unable to reach the NTP baseline (an average BLEU score of 1.55), even in a two-stage setting (with an average BLEU score of 0.63). The experiment increases the vocabulary size by more

1080 Table 6: Benchmark results for Mistral 7B v0.1 with untied embeddings. Training time for "MATT
 1081 w/ NTP (out)" reflects time spent separately on MATT and NTP on output embeddings, respectively.
 1082

1083 1084 1085 1086 1087 1088 1089 1090 1091 1092 1093 1094 1095 1096 1097 1098 1099 1100 1101 1102 1103 1104 1105 1106 1107 1108 1109 1110 1111 1112 1113 1114 1115 1116 1117 1118 1119 1120 1121 1122 1123 1124 1125 1126 1127 1128 1129 1130 1131 1132 1133	1083 1084 1085 1086 1087 1088 1089 1090 1091 1092 1093 1094 1095 1096 1097 1098 1099 1100 1101 1102 1103 1104 1105 1106 1107 1108 1109 1110 1111 1112 1113 1114 1115 1116 1117 1118 1119 1120 1121 1122 1123 1124 1125 1126 1127 1128 1129 1130 1131 1132 1133	Model	Training Time	Long FLORES	WMT	XL-Sum	Avg
Mistral 7B v0.1	-	7.07	1.91	4.12	4.37	-	-
FOCUS	-	0.14	0.06	0.09	0.10	-	-
FOCUS w/ NTP	4h 17m	2.06	0.75	1.85	1.55	-	-
MATT	2h 04m	0.21	0.08	0.40	0.23	-	-
MATT	4h 08m	0.16	0.09	0.37	0.21	-	-
MATT	5h 19m	0.17	0.06	0.38	0.20	-	-
MATT w/ NTP (out)	2h 04m + 2h 32m	0.54	0.59	0.76	0.63	-	-

than five times, drastically changing the model's dynamics, which additionally contributes to why training input and output embeddings jointly is of greater advantage than our two-stage approach. This also leads to a significant performance drop to the point where metrics are close to random generation, preventing a meaningful comparison of certain settings, such as MATT with different compute budgets. We leave designing another experiment with a more favorable configuration for future research.

Another potential way to handle untied embeddings is to follow Token Distillation (Dobler et al., 2025), which combines distillation on the last hidden layer with the NTP objective to optimize both input and output embeddings, albeit at the cost of higher computational requirements.

We also conducted preliminary experiments with a mapping technique that transfers input embeddings to the output embeddings space. In this setup, the output embeddings for new tokens were initialized using the mapped input embeddings after MATT fine-tuning. However, this approach underperformed compared to initializing with FOCUS and then fine-tuning only input embeddings with MATT. This can be attributed to low-capacity mapping models and requires further research.

Despite these early results, the search space remains large, and we believe that more effective strategies for untied embeddings are likely to be found with further exploration.